



**A Method for Utilizing Commercially Available  
Sensors to Investigate Magnetic Field Perturbations  
Associated With Ballistic Events**

**by Thomas Kottke**

**ARL-TR-5625**

**August 2011**

## **NOTICES**

### **Disclaimers**

The findings in this report are not to be construed as an official Department of the Army position unless so designated by other authorized documents.

Citation of manufacturer's or trade names does not constitute an official endorsement or approval of the use thereof.

Destroy this report when it is no longer needed. Do not return it to the originator.

# **Army Research Laboratory**

Aberdeen Proving Ground, MD 21005-5069

---

---

**ARL-TR-5625**

**August 2011**

---

---

## **A Method for Utilizing Commercially Available Sensors to Investigate Magnetic Field Perturbations Associated With Ballistic Events**

**Thomas Kottke**

**Weapons and Materials Research Directorate, ARL**

# REPORT DOCUMENTATION PAGE

*Form Approved*  
OMB No. 0704-0188

Public reporting burden for this collection of information is estimated to average 1 hour per response, including the time for reviewing instructions, searching existing data sources, gathering and maintaining the data needed, and completing and reviewing the collection information. Send comments regarding this burden estimate or any other aspect of this collection of information, including suggestions for reducing the burden, to Department of Defense, Washington Headquarters Services, Directorate for Information Operations and Reports (0704-0188), 1215 Jefferson Davis Highway, Suite 1204, Arlington, VA 22202-4302. Respondents should be aware that notwithstanding any other provision of law, no person shall be subject to any penalty for failing to comply with a collection of information if it does not display a currently valid OMB control number.

**PLEASE DO NOT RETURN YOUR FORM TO THE ABOVE ADDRESS.**

<b>1. REPORT DATE (DD-MM-YYYY)</b> August 2011		<b>2. REPORT TYPE</b> Final		<b>3. DATES COVERED (From - To)</b> October 2010–March 2011	
<b>4. TITLE AND SUBTITLE</b> A Method for Utilizing Commercially Available Sensors to Investigate Magnetic Field Perturbations Associated With Ballistic Events				<b>5a. CONTRACT NUMBER</b>	
				<b>5b. GRANT NUMBER</b>	
				<b>5c. PROGRAM ELEMENT NUMBER</b>	
<b>6. AUTHOR(S)</b> Thomas Kottke				<b>5d. PROJECT NUMBER</b> AH43611102	
				<b>5e. TASK NUMBER</b>	
				<b>5f. WORK UNIT NUMBER</b>	
<b>7. PERFORMING ORGANIZATION NAME(S) AND ADDRESS(ES)</b> U.S. Army Research Laboratory ATTN: RDRL-WMP-A Aberdeen Proving Ground, MD 21005-5069				<b>8. PERFORMING ORGANIZATION REPORT NUMBER</b> ARL-TR-5625	
<b>9. SPONSORING/MONITORING AGENCY NAME(S) AND ADDRESS(ES)</b>				<b>10. SPONSOR/MONITOR'S ACRONYM(S)</b>	
				<b>11. SPONSOR/MONITOR'S REPORT NUMBER(S)</b>	
<b>12. DISTRIBUTION/AVAILABILITY STATEMENT</b> Approved for public release; distribution unlimited.					
<b>13. SUPPLEMENTARY NOTES</b>					
<b>14. ABSTRACT</b> This report presents an architectural framework for utilizing commercially available magnetic sensors to investigate magnetic field perturbations associated with ballistic events. Specifically, the Honeywell HMC1043 three-axis magnetoresistive field sensor is considered along with required circuitry to provide signal offset compensation, signal amplification, and set/reset strap capability. Conditions are quantified for which active offset compensation is desirable, and a method for achieving this compensation is discussed along with the constraints that active compensation imposes on signal amplification. A method for realizing optimal magnetic sensor performance through sensor conditioning set/reset operations is presented. A scheme for integrating an array of 32 HMC1043 magnetic field sensors into a microprocessor-controlled data acquisition and storage system is outlined, and fabrication details are provided.					
<b>15. SUBJECT TERMS</b> magnetic, magnetic field, sensor, ballistic					
<b>16. SECURITY CLASSIFICATION OF:</b>			<b>17. LIMITATION OF ABSTRACT</b>  UU	<b>18. NUMBER OF PAGES</b>  28	<b>19a. NAME OF RESPONSIBLE PERSON</b> Thomas Kottke
<b>a. REPORT</b> Unclassified	<b>b. ABSTRACT</b> Unclassified	<b>c. THIS PAGE</b> Unclassified			<b>19b. TELEPHONE NUMBER (Include area code)</b> (410) 278-2557

---

## Contents

---

<b>List of Figures</b>	<b>iv</b>
<b>List of Tables</b>	<b>iv</b>
<b>Acknowledgments</b>	<b>v</b>
<b>1. Introduction</b>	<b>1</b>
<b>2. Methods for Handling AMR Bridge Offset Voltage</b>	<b>3</b>
2.1 Method 1: Measuring AMR Bridge Offset Effect and Living With It.....	3
2.2 Method 2: Amplifier Bias Nulling Method.....	5
<b>3. Magnetic Sensor Signal Amplification</b>	<b>6</b>
<b>4. Magnetic Sensor Set/Reset Strap</b>	<b>7</b>
<b>5. Electronic Circuitry</b>	<b>9</b>
5.1 Overview .....	9
5.2 Magnetic Sensor Circuitry Details .....	9
5.3 Multiplexing Circuitry.....	13
5.4 Microcontroller and Supporting Circuitry.....	14
<b>6. Summary</b>	<b>16</b>
<b>7. References</b>	<b>17</b>
<b>Distribution List</b>	<b>18</b>

---

## List of Figures

---

Figure 1. Configuration of anisotropic magnetoresistive elements in HMC1043 sensor.....	2
Figure 2. Relative magnitudes of bridge offset and magnetic sensor output voltages. ....	4
Figure 3. Variable reference difference amplifier configuration. ....	6
Figure 4. Schematic of set/reset strap circuitry.....	8
Figure 5. Current flow in strap circuitry during reset (left) and set (right) operations. ....	8
Figure 6. Schematic diagram of magnetic sensor, amplifier, and set/reset components. ....	11
Figure 7. Printed circuit-board layout of magnetic sensor circuitry. ....	12
Figure 8. Schematic diagram of multiplexer circuitry. ....	13
Figure 9. Schematic diagram of microcontroller and supporting components.....	15

---

## List of Tables

---

Table 1. Effect of bridge offset voltage on resolution of earth magnetic field measurements. ....	4
---	---

---

## **Acknowledgments**

---

The author is delighted to acknowledge Dr. George M. Thomson of the U.S. Army Research Laboratory (ARL) Weapons and Materials Research Directorate (WMRD) as the motivating force behind this research effort and thank him for reviewing and improving this manuscript. The author also thanks Barbara E. Ringers (Chief, ARL/WMRD Physics Phenomenology Branch) for supporting every aspect of this project and assisting Jason C. Angel (ARL/WMRD Threat Mechanisms and Modeling Branch) with the manuscript's technical review.

INTENTIONALLY LEFT BLANK.

---

## 1. Introduction

---

The goal of this effort is to provide a foundation for the development of supporting electronic circuitry to facilitate the exploitation of commercially available magnetic sensors for geometric investigations of ballistic components. Specifically, the internal and external geometries of target materials are to be determined through measurements of their perturbations of external magnetic fields. One applicable low-field magnetic sensor is the Honeywell\* HMC1043. This low-cost device contains three orthogonally oriented magnetoresistive field sensors in a miniature  $3 \times 3$ -mm surface-mount device. Magnetic fields up to  $\pm 6$  Oersted (Oe) can be measured with these devices, which is roughly 10 times the earth's magnetic field strength. Consideration of this device's operation will reveal the need for electronic circuitry to provide signal amplification, offset compensation, and set/reset strap capability.

The HMC1043 magnetic sensor utilizes ferrous anisotropic magnetoresistive (AMR) materials. These materials are such that their electrical resistance is a function of both the magnitude and direction of an external applied magnetic field ( $I$ ). Each orthogonally oriented sensor consists of a Wheatstone bridge with elements fabricated from AMR material, as illustrated in figure 1. In this figure, the magnetoresistive orientation direction of each element is indicated by the blue arrow through the resistance symbol. In the absence of an external magnetic field, each Wheatstone bridge element has the same nominal resistance,  $R$ . Under these conditions the bridge is balanced and an externally applied voltage  $V_{CC}$  will generate a bridge voltage of  $\Delta V=0$ . The magnetoresistive elements of the Wheatstone bridge are fabricated such that each diagonal element pair experiences the same sense in resistance variation with applied magnetic field and the sense of the two diagonal pairs is reversed. Therefore, the application of an external magnetic field, shown as red arrows in figure 1, will cause the resistance of one pair of diagonal elements to increase while the other pair of diagonal elements will experience a decrease. This throws the Wheatstone bridge out of balance and a non-zero differential voltage develops at  $\Delta V$ . The magnitude and sense of this differential voltage will depend on the magnitude and direction of the applied magnetic field  $\vec{M}$  and the magnitude and polarity of the applied external voltage  $V_{CC}$ . A nominal device sensitivity of 1.0 mV/V/Oe is specified in the HMC1043 data sheet (2). Thus, at the maximum magnetic field strength of 6 Oe, for an applied Wheatstone bridge voltage of 3.3 V, this sensor will provide an output signal of less than 20 mV. Clearly, some form of signal amplification is desirable. Furthermore, the bipolar, differential nature of the HMC1043 magnetic sensor output suggests the application of a difference amplifier with a quiescent level set at the operating voltage midpoint level,  $V_{cc}/2$ .

---

\*Honeywell, Plymouth, MN, [www.honeywell.com/magneticsensors](http://www.honeywell.com/magneticsensors).

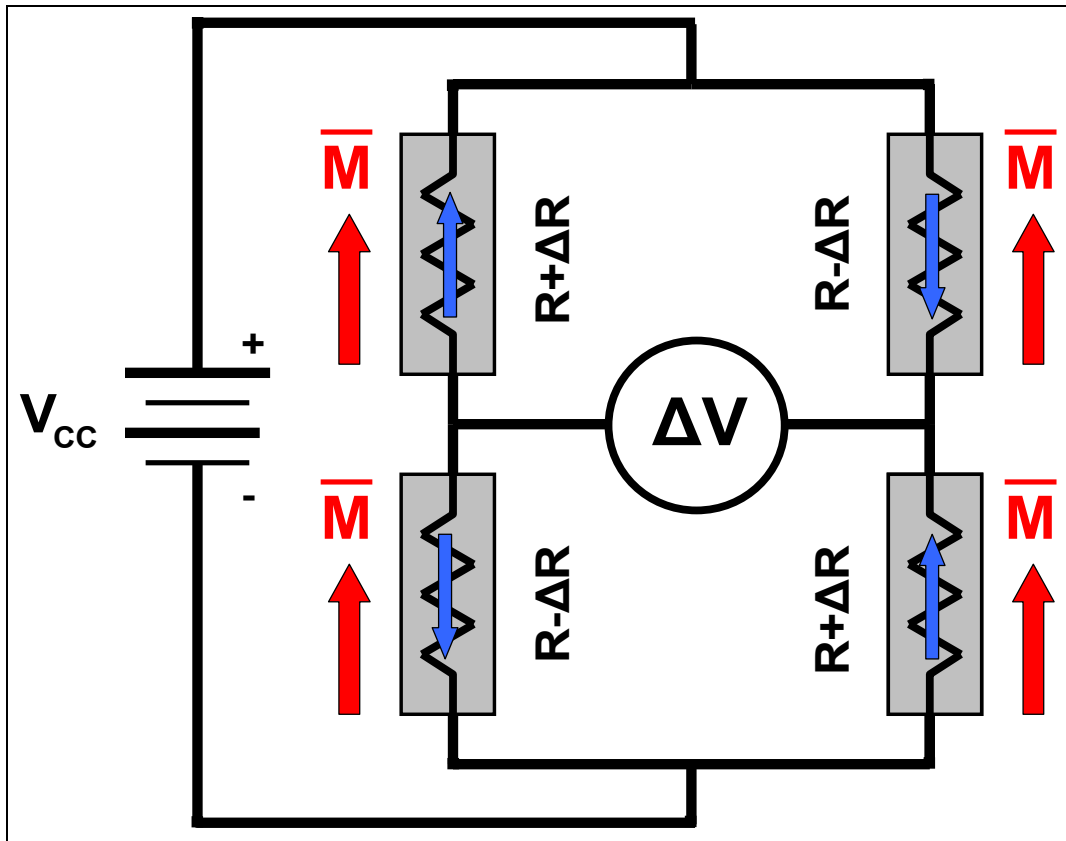


Figure 1. Configuration of anisotropic magnetoresistive elements in HMC1043 sensor.

The previous comment, that in the absence of an external magnetic field each Wheatstone bridge element has the same resistance, is in fact an idealization. The inconvenient reality is variations in fabrication processing result in unavoidable resistive mismatches between Wheatstone bridge elements (3). These resistive variations serve to unbalance the bridge and produce an output voltage even in the absence of externally applied magnetic fields. Two cases for dealing with this zero-stimulus output voltage, known as sensor bridge offset, will be considered. The first approach will be to determine the potential magnitude of the sensor bridge offset and quantify its effect on magnetic field measurement. In essence, this first approach boils down to simply living with the sensor bridge offset. The second approach will be to develop a method for compensating or removing the effects of the sensor bridge offset voltage.

The HMC1043 magnetic sensor also includes a set/reset strap for each orthogonally oriented AMR bridge. This strap consists of a spiral conductor configured to produce a magnetic field. When electrical current is passed through this spiral conductor, it aligns the magnetic domains in the magnetic materials in an orientation that is dependent on the direction of current flow. The set and reset operations refer to the two directions of current flow and the resulting two magnetic domain alignments. These set/reset operations serve multiple purposes. First, periodic set and reset operations prior to magnetic field measurements serve to condition the magnetic domains in the AMR elements by erasing induced magnetization from previously applied external magnetic

fields for optimal performance. Second, toggling between the set and reset states reverses the polarity of magnetic field induced AMR bridge outputs but does not affect the polarity of the bridge offset voltage bias. This second effect is useful in “tuning out” the bridge offset bias.

## 2. Methods for Handling AMR Bridge Offset Voltage

### 2.1 Method 1: Measuring AMR Bridge Offset Effect and Living With It

The HMC1043 data sheet (2) specifies the maximum bridge offset voltage as  $\pm 1.25$  mV/V with a temperature coefficient of  $\pm 10$  ppm/°C. For an assumed temperature operating range of 0 °C to 40 °C, the temperature variations of the bridge offset voltage are negligible. Therefore, for an applied Wheatstone bridge voltage of 3.3 V, the worst case bridge offset voltage is:

$$\text{maximum bridge offset voltage} = (\pm 1.25 \text{ mV/V}) \bullet (3.3 \text{ V}) = \pm 4.1 \text{ mV}. \quad (1)$$

The same data sheet specifies the magnetic sensor sensitivity as  $1.0 \pm 0.2$  mV/V/Oe with a temperature coefficient of  $-3400$  ppm/°C. Over the same assumed temperature operating range, the sensitivity variation is:

$$\text{sensitivity variation over temp. range} = (40 \text{ }^\circ\text{C}) \bullet (-3400 \text{ ppm}/^\circ\text{C}) = -136000 \text{ ppm} = 13.6\%. \quad (2)$$

Therefore, the maximum sensitivity over the chosen temperature range is:

$$\text{maximum sensitivity over temperature range} = (1.136) \bullet (1.2 \text{ mV/V/Oe}) = 1.36 \text{ mV/V/Oe}. \quad (3)$$

The earth’s magnetic field has a maximum value of 0.625 Oe. Thus, for measurements of the earth’s magnetic field using an applied Wheatstone bridge potential of 3.3 V the maximum full-scale magnetic sensor signal is:

$$\text{maximum sensor signal} = (3.3 \text{ V}) \bullet (0.625 \text{ Oe}) \bullet (1.36 \text{ mV/V/Oe}) = 2.8 \text{ mV}. \quad (4)$$

So, under these worst-case scenario conditions, an HMC1043 sensor in the earth’s magnetic field will output signal voltages of  $\pm 2.8$  mV that ride on a bias level that can range from  $-4.12$  to  $+4.12$  mV, depending on the individual component. These signal and offset levels are depicted graphically in figure 2. This illustration highlights the fact that even though the magnetic sensor output signal ranges from only  $-2.8$  to  $+2.8$  mV, the presence of the  $\pm 4.1$  mV bridge offset voltage leads to magnetic sensor output voltages that range from  $-6.9$  to  $+6.9$  mV. So a range of voltages must be amplified and measured for which only 40% correspond to useful sensor signals. This reduces the resolution of subsequent analog to digital conversion (ADC) measurements of the earth’s magnetic field, as listed in table 1. Column (a) of this table lists the number of conversion bits for common ADCs and column (b) lists the number of bins, regions, or allowed values into which each ADC divides the voltage measurement range. Column (c)

provides the corresponding number of useful ADC bits if only 40% of the voltage measurement range corresponds to meaningful magnetic sensor signals. Realizing the earth's magnetic field can range from  $-0.625$  to  $+0.625$  Oe, columns (d) and (e) tabulate the achievable resolutions if the ADCs of columns (b) and (c) are used to measure the earth's magnetic field. The negative effect of the bridge offset voltage on the measured magnetic field resolution is clear.

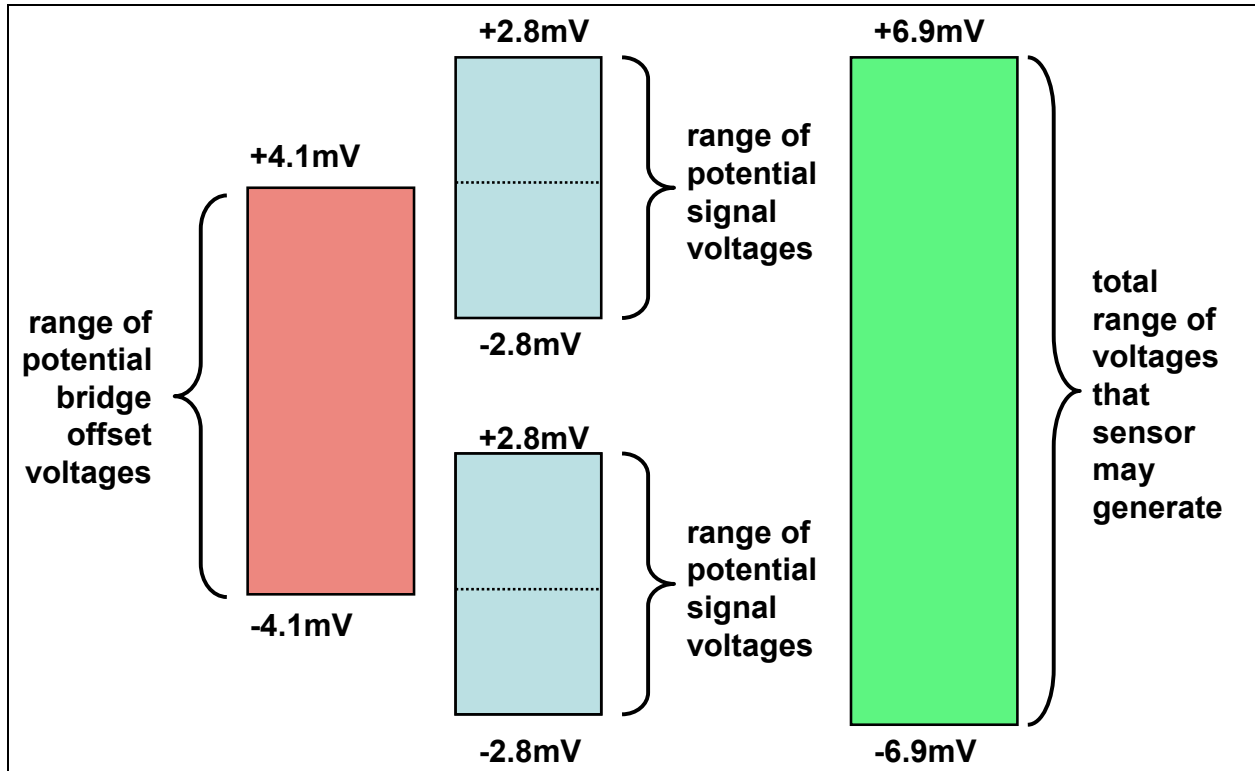


Figure 2. Relative magnitudes of bridge offset and magnetic sensor output voltages.

Table 1. Effect of bridge offset voltage on resolution of earth magnetic field measurements.

(a) Num. of ADC Bits	(b) Num. of ADC Bins	(c) 40% of Num. of ADC Bins	(d) Earth Field Res. w/100% ADC Bins	(e) Earth Field Res. w/40% ADC Bins
8	256	102	4880 $\mu$ Oe	12300 $\mu$ Oe
10	1024	409	1220 $\mu$ Oe	3060 $\mu$ Oe
12	4096	1638	305 $\mu$ Oe	763 $\mu$ Oe

Depending on the application, the tabulated magnetic field measurement resolutions including the undesirable effect of the bridge offset voltage may be sufficient and the strategy of coexisting with this offset voltage may represent a convenient, cost effective solution. However, for applications where magnetic field measurement resolution is critical, some method for compensating or removing the effects of the bridge offset voltage is clearly desirable.

## 2.2 Method 2: Amplifier Bias Nulling Method

One method for compensating magnetic sensor bridge offset voltages is to use a variable reference difference amplifier as illustrated in figure 3. This circuit includes a user adjustable reference voltage  $V_{adj}$  that is available to manually offset the amplifier output voltage  $V_{out}$ . The question then becomes what applied reference voltage  $V_{adj}$  will be required to nullify the effects of the bridge offset voltage? For the condition of zero applied external magnetic field, the two differential outputs from the magnetic sensor's AMR Wheatstone bridge ideally should have the same output voltage  $V_{in}$ . However, the presence of the bridge offset voltage effectively introduces a small bias voltage  $V_{off}$  to one of the magnetic sensor outputs. In the upper portion of figure 3 the differential output voltage  $V_{in}$  is supplied to the voltage divider consisting of upper resistors  $R_1$  and  $R_2$  with a central voltage node at point  $A$  and a termination point at the amplifier output with potential  $V_{out}$ . The voltage at node  $A$  can be expressed as:

$$V_A = V_{in} - (V_{in} - V_{out}) \cdot [R_1 / (R_1 + R_2)]. \quad (5)$$

Similarly, the other differential sensor output voltage  $V_{in} + V_{off}$  is routed to the lower voltage divider with central voltage node at point  $B$  and termination voltage  $V_{adj}$ . The voltage at node  $B$  can be expressed as:

$$V_B = V_{in} + V_{off} - (V_{in} + V_{off} - V_{adj}) \cdot [R_1 / (R_1 + R_2)]. \quad (6)$$

In the difference amplifier configuration shown in figure 3, the operational amplifier will drive the output voltage  $V_{out}$  to make the potentials at the input nodes  $A$  and  $B$  equal. Therefore, equating equations 5 and 6:

$$V_{in} - (V_{in} - V_{out}) \cdot [R_1 / (R_1 + R_2)] = V_{in} + V_{off} - (V_{in} + V_{off} - V_{adj}) \cdot [R_1 / (R_1 + R_2)]. \quad (7)$$

Eliminating like terms and multiplying through by  $(R_1 + R_2)$  equation 7 reduces to:

$$V_{out} \cdot R_1 = V_{off} \cdot (R_1 + R_2) - (V_{off} - V_{adj}) \cdot R_1. \quad (8)$$

Notice the common mode magnetic sensor output voltage  $V_{in}$  does not appear in equation 8. This is as expected for a difference amplifier where only the difference between the two input voltages is amplified. Solving for the amplifier output voltage:

$$V_{out} = V_{adj} + V_{off} (R_2 / R_1). \quad (9)$$

Equation 9 reveals the undesirable effect of the bridge offset voltage  $V_{off}$  on the quiescent output voltage  $V_{out}$  can be nullified by applying a reference potential  $V_{adj}$  that is opposite in sign to the offset voltage and amplified by the ratio of  $R_2$  to  $R_1$ .

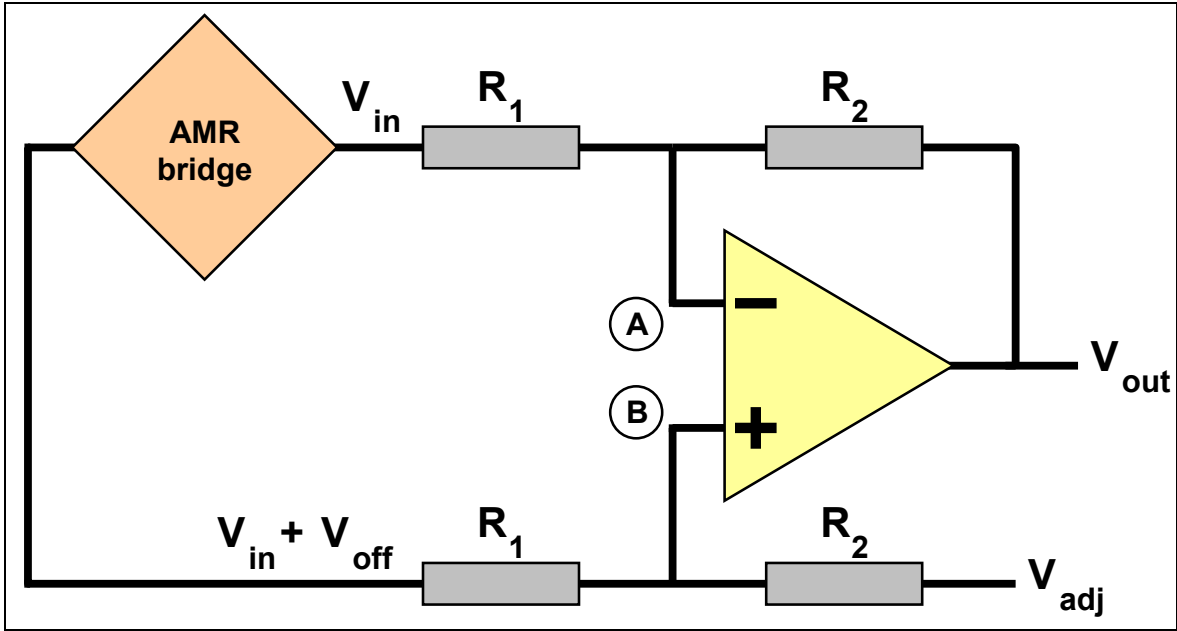


Figure 3. Variable reference difference amplifier configuration.

### 3. Magnetic Sensor Signal Amplification

The ratio of resistor value  $R_2$  to resistor value  $R_1$  in equation 9 is also the amplification of the difference amplifier shown in figure 3. Equation 9 sets a limiting condition on the value of  $R_2/R_1$  and therefore on the allowed amplification value for this stage of amplification. For optimal operation, the desired quiescent output voltage  $V_{out}$  is half of the source voltage  $V_{CC}$ . Also, the applied reference potential  $V_{adj}$  can have minimum and maximum values of  $0$  and  $V_{CC}$  respectively. Substituting these values into equation 9, the maximum amplification factor that will allow all possible bridge offset voltage values to be compensated is:

$$\text{maximum amplification factor} = R_2 / R_1 = (V_{CC} / V_{off}) / 2. \quad (10)$$

For a source voltage of 3.3 V and magnetic sensor bridge offset voltages of 4.1 mV, this difference amplifier's maximum amplification factor is limited to about 400. In practice, it may be desirable to employ a lower amplification level with additional signal amplification provided by subsequent stages of amplification.

---

## 4. Magnetic Sensor Set/Reset Strap

---

As discussed in the introduction, the HMC1043 set/reset strap provides a method for obtaining optimal sensor performance and toggling the sense of the sensor's output with applied magnetic field. For the set and reset operations, electrical currents must be passed through the conductive strap coil in alternate directions. A circuit for providing these electrical currents is displayed in figure 4. The central component in this figure is a field effect transistor (FET) pair consisting of complementary n-channel *c* and p-channel *b* components. A common gate is connected to a logic switch *a*. In the quiescent state, this gate is held high which drives the p-channel components into nonconduction and the n-channel component into conduction.

In this configuration, the source voltage  $V_{CC}$  charges capacitor *e* through the current limiting isolation resistor *d* while the n-channel FET drains any excess charge from capacitor *f*. When the logic switch is grounded, the conduction states of the complementary FET pair are reversed. Charge from capacitor *e* is then allowed to flow to capacitor *f* resulting in a flow of positive current through the strap coil in a clockwise direction, as illustrated in the left-hand portion of figure 5.

When the common FET gate is subsequently returned to the quiescent high level, the FETs once again reverse their conduction state, the positive charge on capacitor *f* is shorted to ground through the n-channel FET, and positive current flows through the strap coil in a counter clockwise direction to neutralize the remaining negative charge on capacitor *f*. Thus, the required set/reset alternating current through the strap coil can be generated by rapidly grounding and then pulling high the common FET gate, *a*.

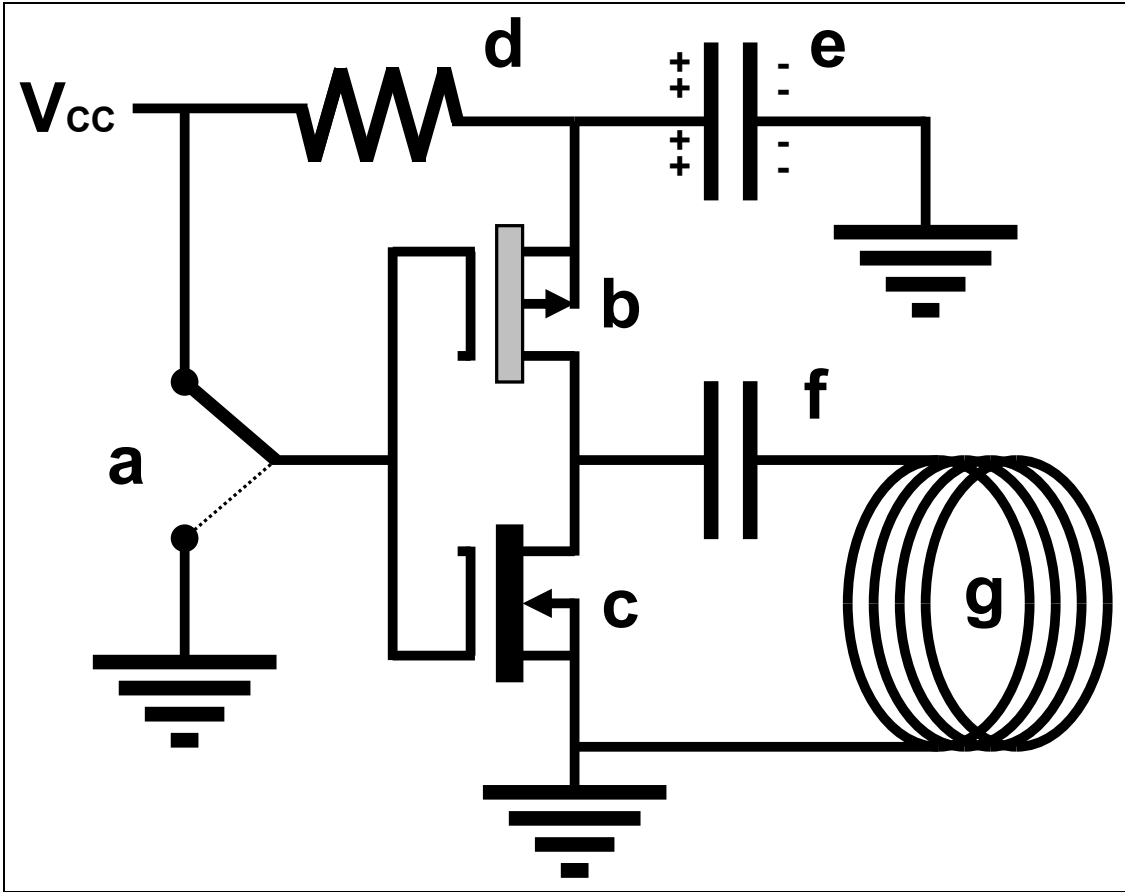


Figure 4. Schematic of set/reset strap circuitry.

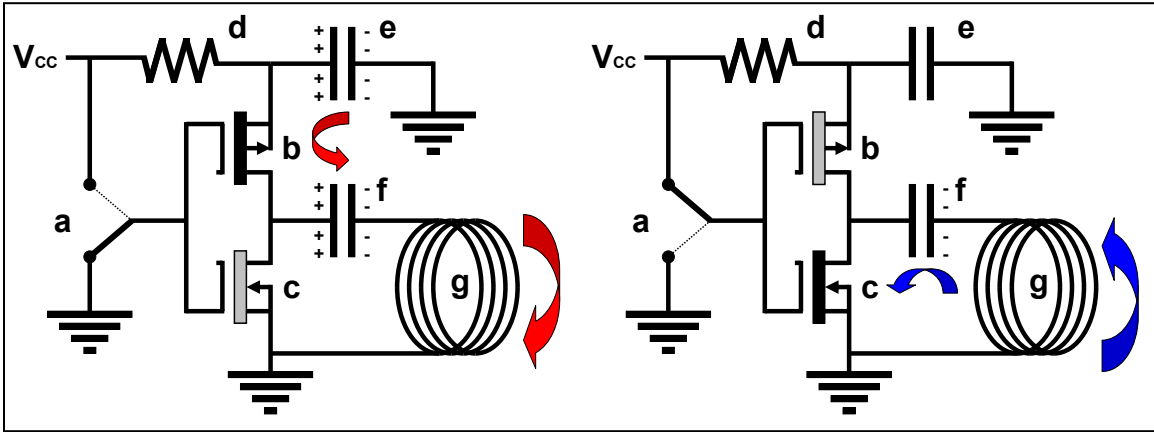


Figure 5. Current flow in strap circuitry during reset (left) and set (right) operations.

The HMC1043 data sheet (2) specifies required strap currents of 1 A for a minimum time interval of 2  $\mu$ S. For the nominal strap coil resistance of 2.5  $\Omega$ , a source potential of 3.3 V is capable of supplying the required current. Assuming a conservative current flow time of 5  $\mu$ S, the charge that must be supplied by the storage capacitors is:

$$q = I \cdot t = (1 \text{ C/S}) \cdot (0.000005 \text{ S}) = 0.000005 \text{ C} . \quad (11)$$

For the 3.3-V source voltage, the minimum size of the storage capacitors is:

$$C = q/V = (0.000005 \text{ C})/(3.3 \text{ V}) \cong 1.5 \mu\text{F} . \quad (12)$$

Therefore, readily available 4.7- $\mu$ F ceramic capacitors with low equivalent series resistance can easily supply the required strap currents.

---

## 5. Electronic Circuitry

---

### 5.1 Overview

A system is presented that is capable of accessing 32 independent HMC1043 magnetic sensors to monitor a three-dimensional magnetic field over an extended volume. First, the circuit details of the magnetic sensors and their local supporting components will be described. Then multiplexing circuitry will be introduced that allows the multiple magnetic sensors to access a limited number of DAC channels for signal-level measurement. Finally, the microcontroller that controls and coordinates the activities of the magnetic field measurement system will be discussed.

### 5.2 Magnetic Sensor Circuitry Details

A schematic diagram of a single magnetic sensor and its local supporting components is illustrated in figure 6. This schematic highlights the components contained at every magnetic sensor site. The magnetic sensor is located in the upper-left portion of this figure. Differential outputs from each of the three orthogonal measurement directions are routed to separate operational amplifiers located on the right side of this figure. As shown, these differential signals are amplified by a factor of 100, but these amplification factors can be easily varied by changing the values of the input and feedback resistive component. The operational amplifier in the lower-right portion of the figure buffers the user adjustable reference voltage  $V_{ADJ}$  that is available to manually offset the effects of the bridge offset voltages.  $V_{ADJ}$  is a common voltage that is simultaneously supplied to all the differential amplifiers for all the measurement directions of all the magnetic sensors. Therefore, before each component of the magnetic field at the location of each magnetic sensor is measured,  $V_{ADJ}$  must be adjusted to a previously determined voltage value that compensates for the particular bridge offset voltage of the AMR Wheatstone bridge being used to perform the measurement. Thus, the optimal  $V_{ADJ}$  needs to be determined in advance for each orthogonally oriented bridge in each magnetic sensor and stored in a readily

accessible look-up table. This process can be handled by an automated calibration routine. The good news is that bridge offset voltages remain the same during the lifetime of the magnetic sensor (3). Therefore, the appropriate reference voltages for each magnetic sensor only need to be measured and stored once. The four operational amplifiers in this circuit are contained in a single LMV324 low-cost, low-power, input/output rail-to-rail quad package (4).

The circuitry in the lower-left portion of figure 6 provides the current pulses for the set and reset operations. A common *SET* signal is supplied to all 32 magnetic sensors to simultaneously perform the set/reset operation. This *SET* signal is provided by the microcontroller. The complementary n and p channel FET pair is contained in a single FDC6420C package (5).

It is desirable to have the printed circuit board (PCB) footprint of the circuitry in figure 6 be as small as possible so the magnetic sensors can be closely spaced for maximum spatial resolution of the magnetic field measurement. Figure 7 illustrates a suggested layout for the magnetic sensor components shown schematically in figure 6.

The four layers of the PCB are displayed individually as well as a composite image shown to scale at the center. Layer 1 includes the digital set/reset components, the magnetic sensor, and a digital ground plane. Layer 4 contains the analog amplification components and an analog ground plane. Layers 2 and 3 are inner layers dedicated to interconnect traces and digital and analog power planes respectively. The full-scale image at the center of figure 7 reveals the PCB footprint that allows magnetic sensors to be placed as close as 0.6 inch on center.

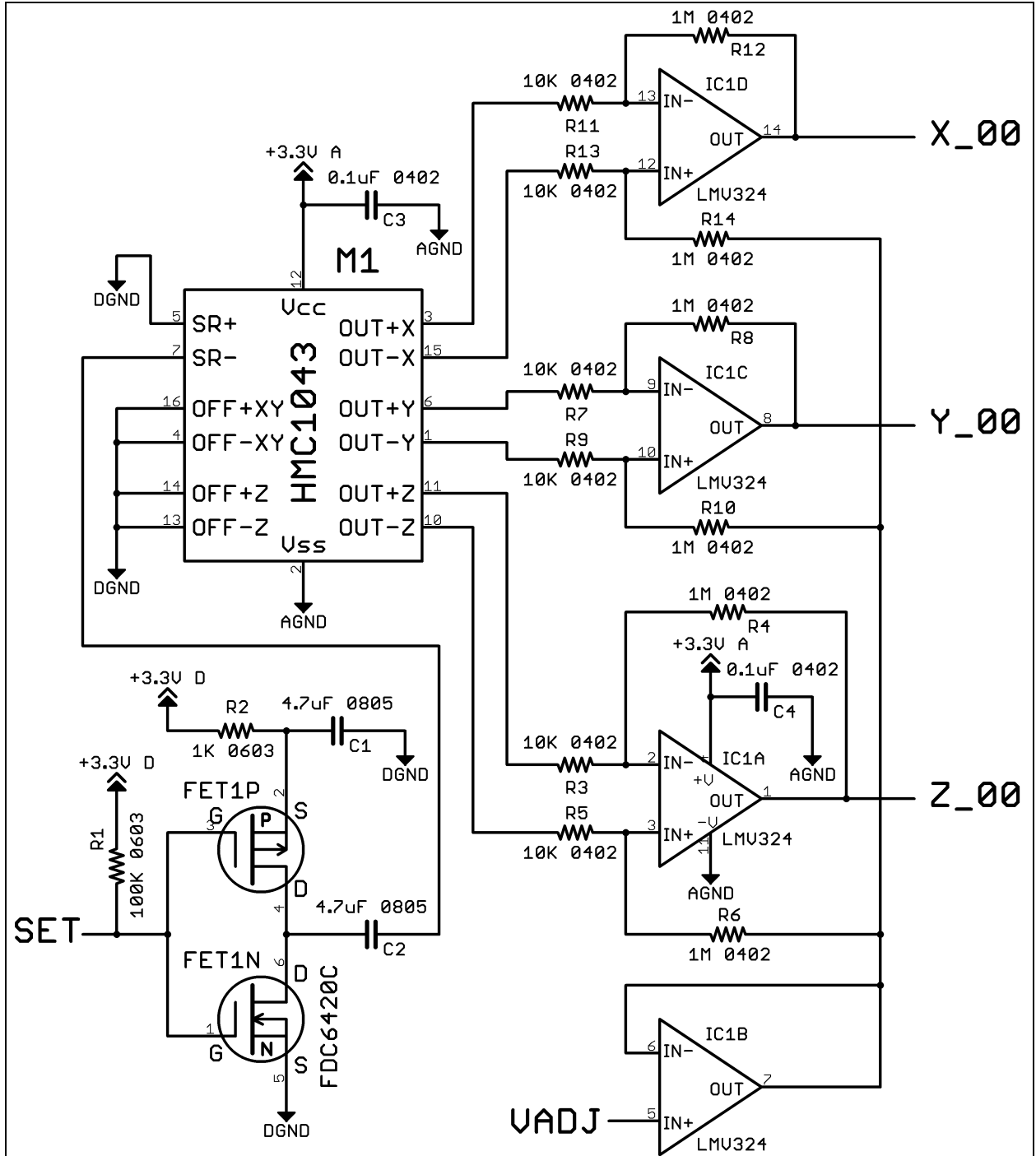


Figure 6. Schematic diagram of magnetic sensor, amplifier, and set/reset components.

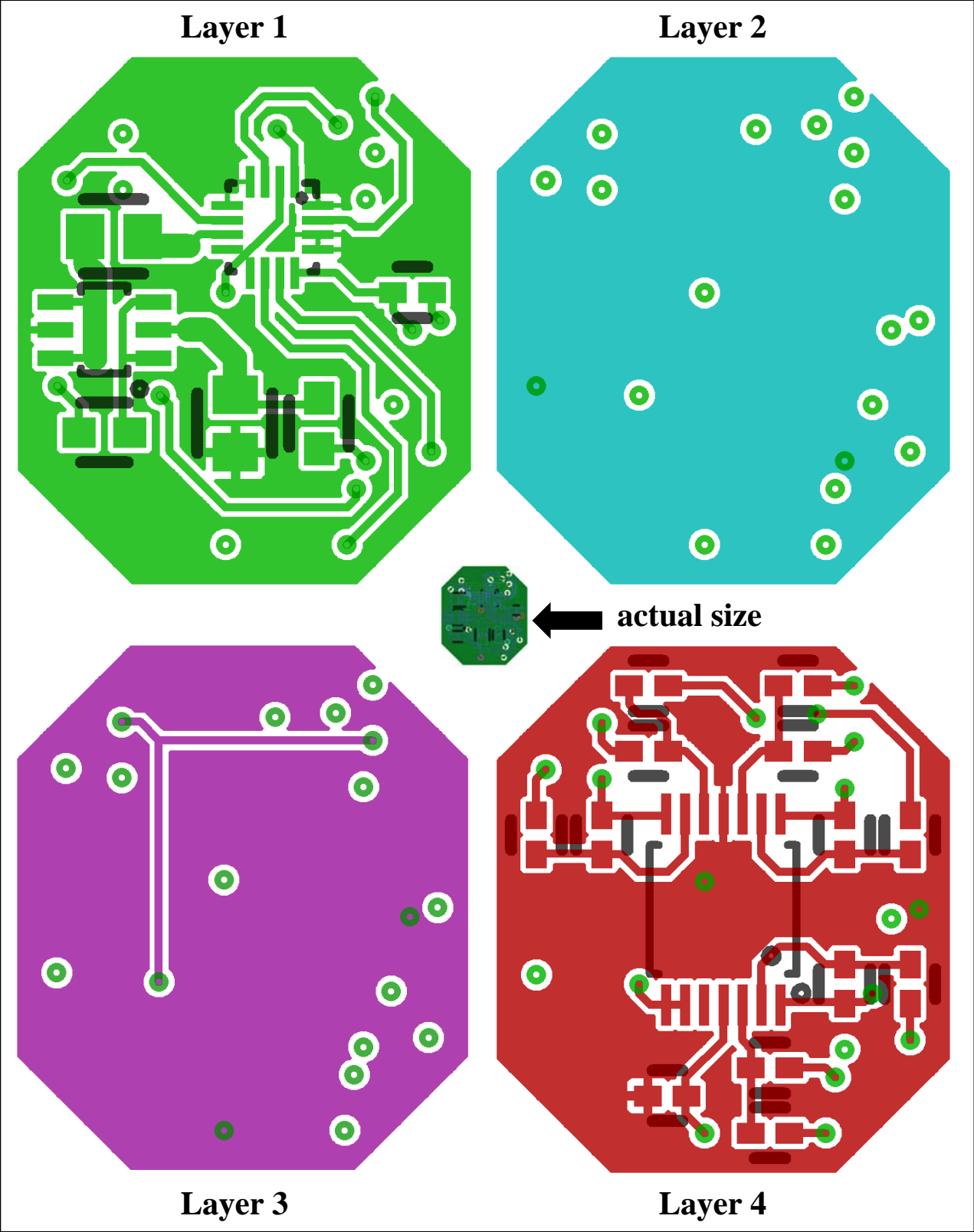


Figure 7. Printed circuit-board layout of magnetic sensor circuitry.

### 5.3 Multiplexing Circuitry

To provide a separate ADC channel for each of the 96 signals generated by an array of 32 magnetic sensors would be a significant burden. To avoid this encumbrance, multiplexers are utilized to reduce the required number of ADC inputs. As illustrated in figure 8, each of the x-axis magnetic field measurement signals from all 32 magnetic sensors is routed to a single ADG732 32-to-1 analog multiplexer (6). Similarly, each of the y-axis signals are routed to an ADG732 and the same for the z-axis magnetic field measurement signals. The use of three 32-to-1 multiplexers reduces the required number of ADC input channels from 96 to just 3. For each of the multiplexers, selection of which magnetic sensor signal is passed through to the  $ADC\_*$  output is determined by the values of the address-selection lines,  $ADD0$  through  $ADD4$ . After the desired address value is placed on the address selection lines, control lines  $WR\_*$  and  $CS\_*$  are used to latch the address value into the analog multiplexer. Additionally, the  $EN\_*$  control line is used to enable or disable the multiplexer. When disabled, none of the 32 input signals are passed through to the output pin. All control and address lines are managed by the microcontroller.

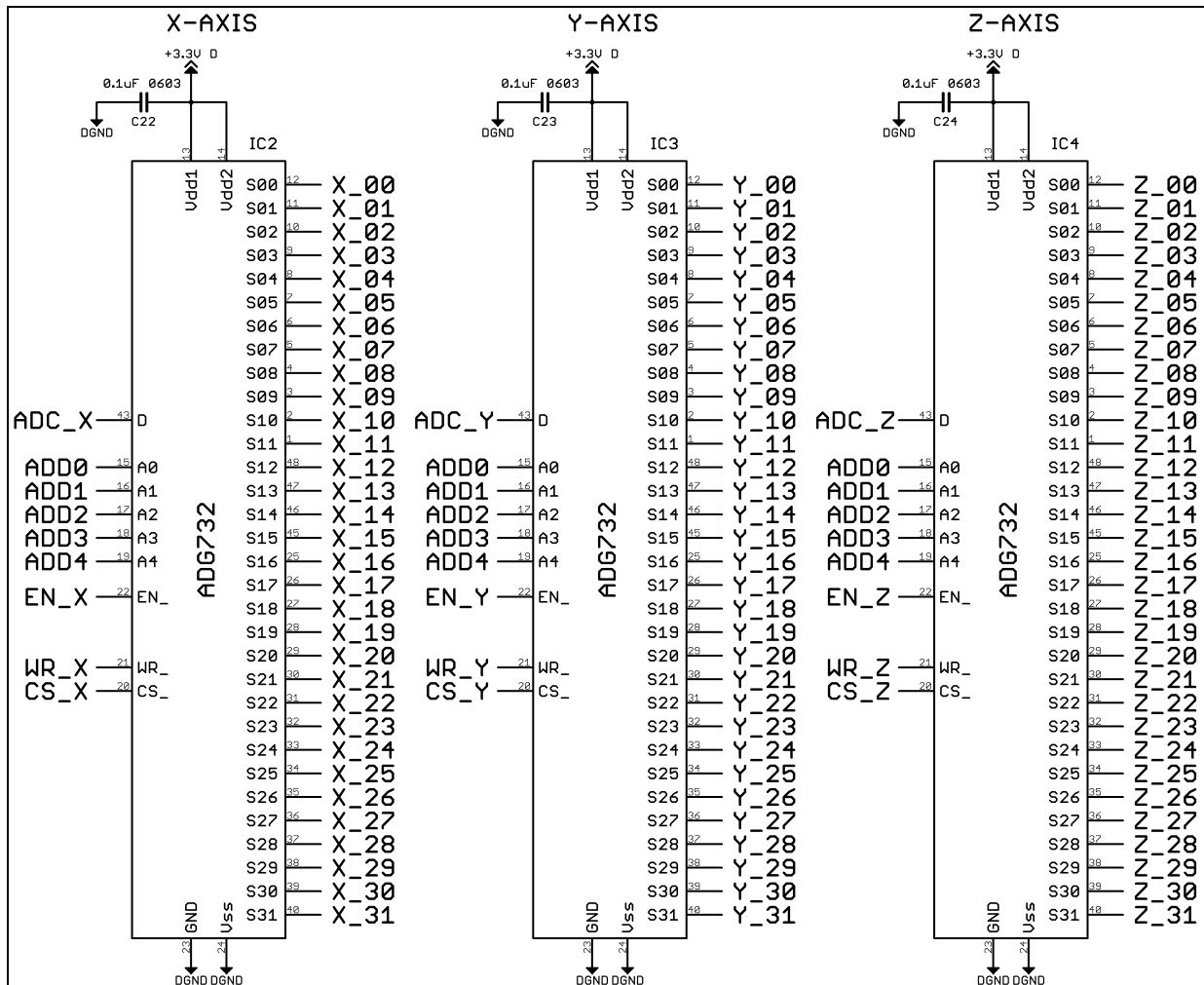


Figure 8. Schematic diagram of multiplexer circuitry.

## 5.4 Microcontroller and Supporting Circuitry

A suitable microcontroller that is capable of coordinating and controlling the activities of this magnetic field measurement system is the Microchip\* PIC24HJ256GP210A. This high-end, 16-bit microcontroller combines a wide variety of peripherals with a considerable amount of program and data-storage capability in a single package. With a processing speed of 40 million instructions per second and a user-friendly integrated development environment, the PIC24HJ256GP210A can serve as a flexible platform for current development as well as future enhancements. This microcontroller and its supporting components are illustrated schematically in figure 9.

The array of capacitors at the top of figure 9 serves to condition the voltage sources that power the microcontroller. High-frequency noise on these power lines can be mitigated by placing decoupling capacitors near every pair of microcontroller power supply pins on the PCB (7). Continuing clock-wise around the microcontroller symbol on figure 9, digital pins from register D provide the  $ADD\#$ ,  $EN\_*$ ,  $WR\_*$ , and  $CS\_*$  control signals for determining which magnet sensor signals pass through the previously discussed multiplexers. A MAX3232 RS-232 line driver/receiver converts the unipolar 3.3-V signals from the microcontroller number 1 serial port to bipolar signals that allow acquired magnet field data to be transferred to a personal computer for long-term storage, analysis, and display (8).

The user-adjustable reference voltage  $V_{adj}$  that is used to manually offset the amplifier output voltage  $V_{out}$  is generated using the microcontroller's three-wire serial peripheral interface (SPI), and an AD5160 SPI compatible digital potentiometer (9). An operational amplifier is used to buffer the digital potentiometer output. In the lower-right corner the input and output pins from the microcontroller's second RS-232 serial port are made available for future wireless interfacing. Working up the right side of the microcontroller symbol, there are more decoupling capacitors. The  $ADC\_*$  lines of register C are the three analog-to-digital inputs that interface with the analog outputs from the three multiplexers. Lines  $M$ ,  $V$ ,  $G$ ,  $D$ , and  $C$  make up the in-circuit programming port that allows the microcontroller's program memory to be programmed, erased, and reprogrammed as required. Four external interrupt lines are available to coordinate and alter program execution with external events. Finally, a CWX813 10-mHz clock is used to drive and pace the internal workings of the microcontroller (10).

---

\*Microchip Technology Inc., Chandler, AZ, [www.microchip.com](http://www.microchip.com).

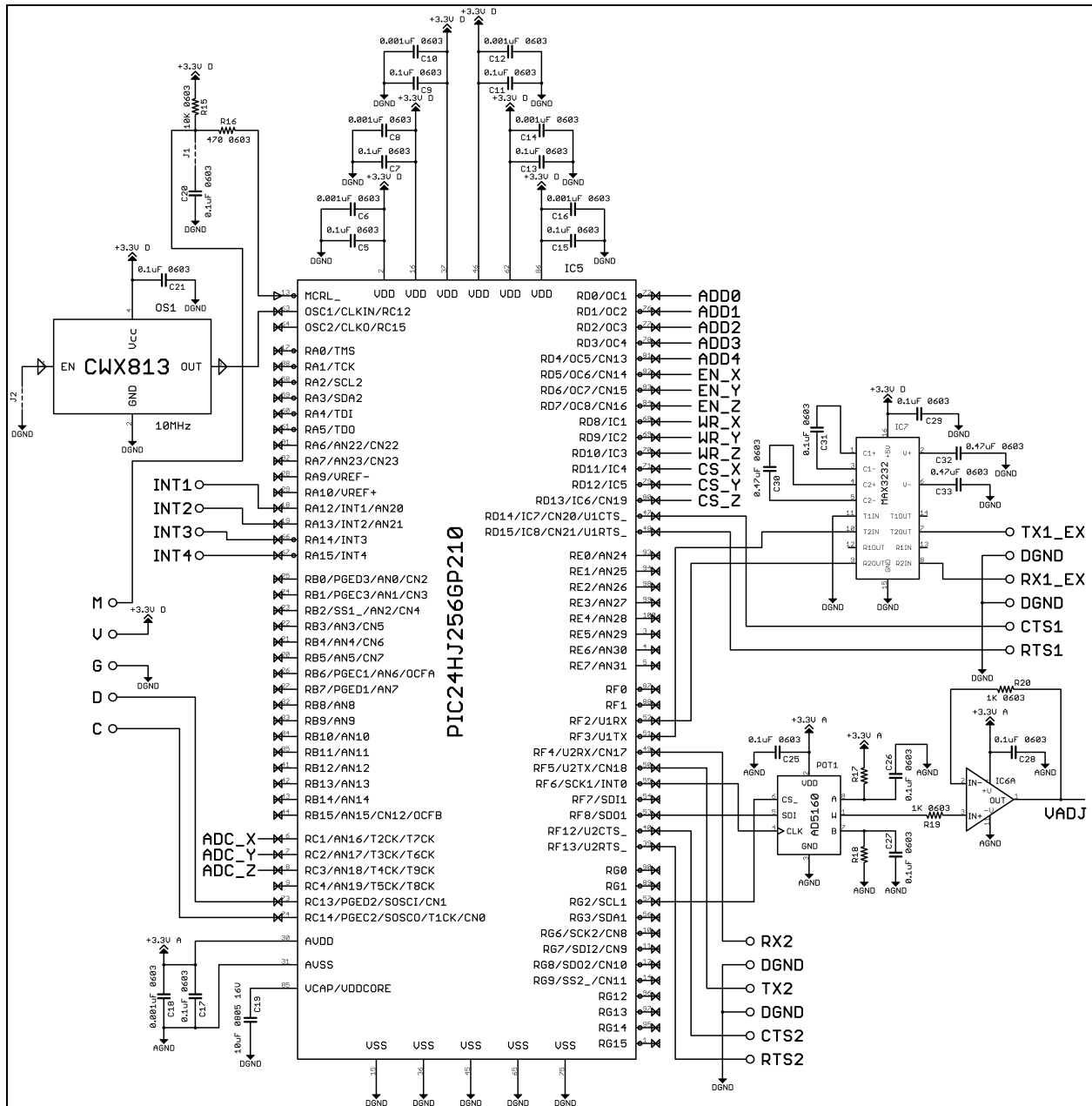


Figure 9. Schematic diagram of microcontroller and supporting components.

---

## 6. Summary

---

This report presents an architectural framework for utilizing commercially available magnetic sensors to investigate magnetic field perturbations associated with ballistic events. Specifically, the Honeywell HMC1043 three-axis magnetoresistive field sensor is considered along with required circuitry to provide signal offset compensation, signal amplification, and set/reset strap capability. Conditions are quantified for which active offset compensation is desirable and a method for achieving this compensation is discussed along with the constraints that active compensation imposes on signal amplification. A method for realizing optimal magnetic sensor performance through sensor conditioning set/reset operations is presented. A scheme for integrating an array of 32 HMC1043 magnetic field sensors into a microprocessor-controlled data acquisition and storage system is outlined and fabrication details are provided.

---

## 7. References

---

1. *Applications of Magnetic Position Sensors*, Honeywell Application Note AN211, available at [www.magneticsensors.com](http://www.magneticsensors.com), accessed September 2010.
2. *3-Axis Magnetic Sensor HMC1043*, Honeywell publication Form #900341 Rev D, October, 2008, available at [www.honeywell.com/magneticsensors](http://www.honeywell.com/magneticsensors), accessed September 2010.
3. *Handling Sensor Bridge Offset*, Honeywell Application Note AN212, available at [www.magneticsensors.com](http://www.magneticsensors.com), accessed September 2010.
4. *LMV321, LMV358, LMV324 Low Cost, Low Power, Input/Output Rail-To-Rail Operational Amplifiers*, STMicroelectronics data sheet Doc ID 11887 Rev 4, available at [www.st.com](http://www.st.com), accessed December 2010.
5. *FDC6420C 20V N & P-Channel PowerTrench MOSFETS*, Fairchild Semiconductor data sheet FDC6420C Rev CW, available at [www.fairchildsemi.com/pf/FD/FDC6420C.html](http://www.fairchildsemi.com/pf/FD/FDC6420C.html), accessed December 2010.
6. *ADG726/ADG732 16-/32-Channel, 4Ω +1.8 V to +5.5 V, ±2.5 V Analog Multiplexers*, Analog Devices data sheet ADG726/ADG732, available at [www.analog.com](http://www.analog.com), accessed December 2010.
7. *PIC24HJXXXGPX06A/X08A/X10A Data Sheet, High-Performance, 16-bit Microcontroller*, Microchip Technology data sheet DS70592B, available at [www.microchip.com](http://www.microchip.com), accessed December 2010.
8. *3.0V to 5.5V, Low-Power, up to 1Mbps, True RS-232 Transceivers Using Four 0.1μF External Capacitors*, Maxim Integrated Products data sheet 19-0273; Rev 7 January 2007, available at [www.maxim-ic.com](http://www.maxim-ic.com), accessed December 2010.
9. *256-Position SPI-Compatible Digital Potentiometer*, Analog Devices, Inc. data sheet AD5160, Rev B, available at [www.analog.com](http://www.analog.com), accessed December 2010.
10. *5.0 x 7.0 Surface Mount CMOS Clock Oscillator Series*, Connor-Winfield, Corp. data sheet Sm126, Rev. 01, May 2009, available at [www.conwin.com](http://www.conwin.com), accessed December 2010.

NO. OF  
COPIES ORGANIZATION

1 DEFENSE TECHNICAL  
(PDF INFORMATION CTR  
only) DTIC OCA  
8725 JOHN J KINGMAN RD  
STE 0944  
FORT BELVOIR VA 22060-6218

1 DIRECTOR  
US ARMY RESEARCH LAB  
IMNE ALC HRR  
2800 POWDER MILL RD  
ADELPHI MD 20783-1197

1 DIRECTOR  
US ARMY RESEARCH LAB  
RDRL CIO LL  
2800 POWDER MILL RD  
ADELPHI MD 20783-1197

1 DIRECTOR  
US ARMY RESEARCH LAB  
RDRL CIO MT  
2800 POWDER MILL RD  
ADELPHI MD 20783-1197

1 DIRECTOR  
US ARMY RESEARCH LAB  
RDRL D  
2800 POWDER MILL RD  
ADELPHI MD 20783-1197

NO. OF  
COPIES ORGANIZATION

ABERDEEN PROVING GROUND

24 DIR USARL  
RDRL WMP A  
J BALL  
P BERNING  
I BILOIU  
J FLENIKEN  
C HUMMER  
T KOTTKE (6 CPS)  
A NIILER  
A PORWITZKY  
J POWELL  
B RINGERS  
G THOMSON  
W UHLIG  
T VALENZUELA  
C WOLFE  
RDRL WMP B  
C HOPPEL  
B LEAVY  
RDRL WMP C  
T BJERKE  
R MUDD  
RDRL WMP D  
J RUNYEON

INTENTIONALLY LEFT BLANK.